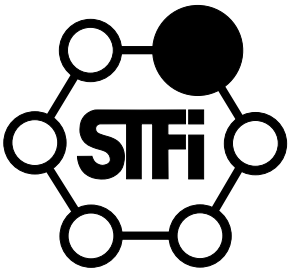

Combined shear and compression analysis using a modification of the Iosipescu shear test device

Federica De Magistris

Stockholm 2003
Royal Institute of Technology
Department of Mechanics
SE-100 44 Stockholm, Sweden

Punta sempre alla luna,
male che vada
avrai vagabondato fra la stelle.

(Daniel Pennac)

Abstract

The mechanical treatment of wood in a refiner is a complex combination of shear and compression forces. To obtain more knowledge on this mechanical treatment, a new fixture was developed to test the behavior of wood under a combined shear and compression load. In this fixture different combinations of shear and compression load were possible to achieve by different rotations of the shear test device.

Measurements were made using both an original (Wyoming version) and an in-house modified fixture based on the Iosipescu shear test. A medium density fiberboard (MDF) was used in order to examine the behavior of the modified device with an orthotropic material without the complexity of the annual ring structure of wood. The MDF was tested in the three main orientations both in tension and in shear. Numerical simulation of the combined shear and compression test was carried out to verify the reliability of the modified device. The numerical results showed good agreement with the experimental results for the shear test in all the three material directions tested. The shapes as well as the values of the strain fields were similar in the numerical and experimental results. Different rotations of the combined shear and compression device were studied using the Finite Element model to find the combinations that gave reliable results in shear and compression. It was found that the 45 ° rotation gave the most uniform strain fields in the section between the notches. This rotation was then tested on the fiberboard and, again, the experimental results were compared with the numerical ones.

Experiments were then made on dry wood using the modified device in the 45 ° rotation. Numerical simulations of the combined shear and compression test were carried out to verify the reliability of the modified device applied to wood. The analysis showed that wood exhibits a non-linear material behavior under combined shear and compression load. Probably non-linear material behavior of the wood cells appears in the supposedly elastic range of the material due to this combination of shear and compression forces.

Keywords: Combined shear and compression, Iosipescu shear test device, Medium Density Fiberboard, spruce (*Picea abies*).

List of papers

The thesis is based upon the following manuscripts:

A. Federica De Magistris, Lennart Salmén *Combined shear and compression analysis using the Iosipescu device. Analytical and experimental studies of medium density fiberboard*
Submitted to Wood Science and Technology

B. Federica De Magistris, Lennart Salmén *Combined shear and compression analysis using a modification of the Iosipescu shear test device. Analytical and experimental studies on dry wood*
Submitted to Holzforschung

Contents

1 Introduction

In mechanical pulping, wood fibers are repeatedly sheared and compressed at high temperatures in order to make them suitable for use in papermaking pulps. This loading perpendicular to the fiber axis results in fiber collapse, which is desirable for making fibers more flexible. Measurements in shear and compression of wood are desired in order to gain more information regarding the possibilities of affecting that process in order to make it more energy efficient.

The objective of this work has been to develop a testing device to be able to test wood in shear and compression and evaluate the behavior of wood under a combination of these.

For this purpose a testing device, based on the Iosipescu shear test, was developed. Two materials were tested, a Medium Density Fiberboard (MDF) and a spruce wood sample (*Picea abies*). The MDF was used to check the behavior of the shear and compression device applying an orthotropic homogeneous material with mechanical characteristics close to those of wood.

1.1 Background

A variety of test methods exist for introducing shear stresses in materials. However, all these tests methods posses some disadvantage, making them less than ideal.

The most uniform shear-stress state can be achieved in a material by applying torsional loading to a thin walled tube specimen (Feldman et al. 1966). However tubular specimens are usually expensive. Several test methods are currently used for determining shear properties of flat test specimens. The ideal test method is one that is relatively simple to conduct and requires small and easily fabricated specimens.

When trying to combine deformation in shear and compression the problem becomes even more difficult. Due to the fact that it is much more difficult to achieve pure shear than pure compression, a shear method with the possibility to be developed to a combined shear and compression test was chosen here. Just two methods were found suitable to use in combined shear and compression: the Arcan and the Iosipescu methods.

Arcan et al. (1978) developed a method for testing shear properties of composite materials under uniform plane-stress conditions by means of a

specially designed butterfly-shaped specimen. Liu (1984) tested this method on wood.

The Iosipescu shear test method (1967) was originally designed for determining shear properties of metals. It uses an asymmetrically loaded notched beam to generate a pure shear strain field in the section between the notches. Walrath and Adams (1983) introduced a fixture that has extended the Iosipescu shear test method to composite materials. In the literature this fixture is called the Wyoming fixture. This modification of the Iosipescu shear method is the most used shear test method for composite materials (Grédiac et al. 1994, Liu 2000). The test method can provide results for both the shear modulus and the shear strength (Walrath and Adams 1983). However, more recent studies have shown that special care should be taken if a more precise estimate of the shear properties is required. When testing orthotropic materials, off-axis effects have been seen and different developments of the Iosipescu shear test device have been proposed (Liu et al. 1999, Conant and Odom 1995). Bansal and Kumosa (1995) have extended the traditional Iosipescu shear test to a biaxial fixture to characterize mixed-mode failure phenomena of both isotropic and orthotropic materials.

In the Iosipescu shear test the sample is clamped in a mechanical way to the fixture while for the Arcan it is necessary to glue the wood sample to the support. This can cause a lot of problems with penetration of the glue. Mainly for this reason the Iosipescu shear test was chosen to be developed in a shear and compression method.

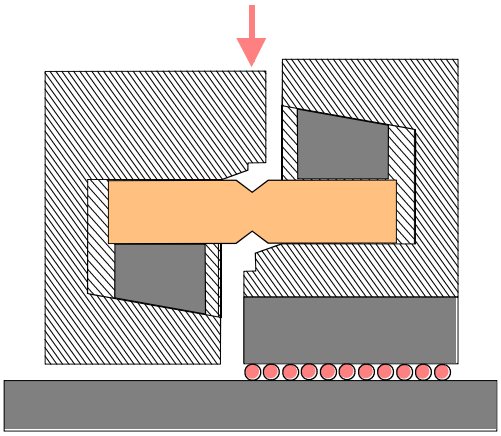

Figure 1: Wyoming version of the Iosipescu shear test device.

2 Development of the testing device

The Iosipescu shear testing device was chosen as the basis for the development of a combined testing of shear and compression. An in-house modification of the Iosipescu shear test device was developed. This modification is based on the Wyoming version of the Iosipescu shear test fixture (Adams and Walrath 1987), see **Figure 1**.

The idea of the modification consists in the possibility to rotate the jaws to make it possible to achieve a combination of shear and compression forces with a purely vertical movement of the piston of the hydraulic tensile testing machine (MTS), **Figure 2**.

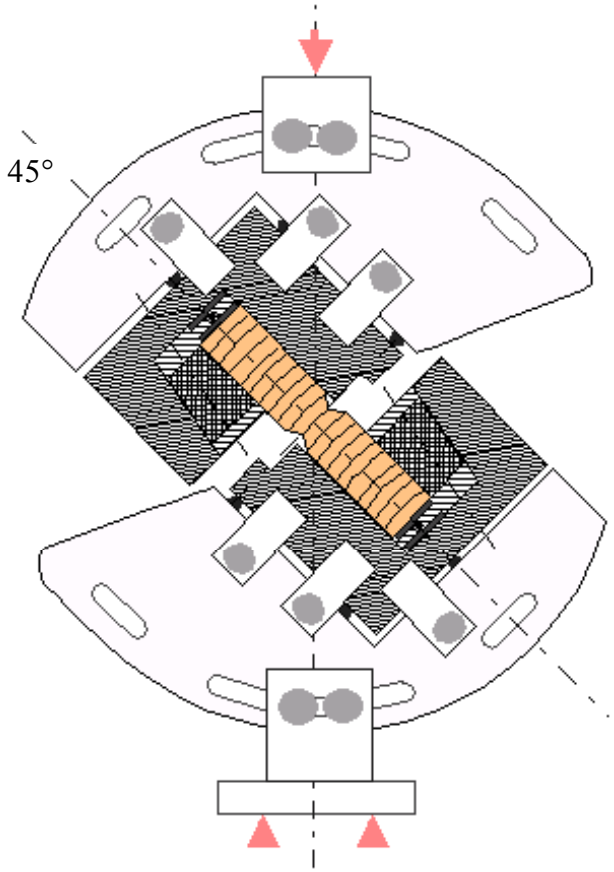

Figure 2: New test setting for the combined shear and compression device.

A number of studies using the Wyoming fixture have reported results that indicate that the test method is not always functioning as expected (Conant and Odom 1995):

- The compliance of the two halves of the fixture was found unequal.
- Unequal shear strains on the front and back of the specimen show that the specimen twists.
- Inability to obtain the same shear-strain response with repeated series of tests.

The design criteria for the modified fixture thus required that the modification, other than to fulfill the main experimental purpose, should have the following characteristics:

- The fixture halves should be physically identical.
- The fixture should prevent misalignment of the two halves.
- Lateral support of the sample should be introduced.

In order to fulfill these requirements, the two halves were connected in a way that the center of the sample was fixed in space independent of the rotation of the halves themselves. The two supports were identical as was the connection with the testing machine. Alignment of the two halves was checked before every test. Two adjustable supports were introduced between the lateral edges of the samples and the fixture to transmit the compression directly to the edge of the sample and not through the griping sections.

3 Materials

3.1 Medium Density Fiberboard

Medium Density Fiberboard (MDF) with a thickness of 32 mm was used. The thickness of the board ensured that the material properties were homogeneous in the region from which specimens were cut. The three principal directions of the material were denoted A, B, and C. The fibers lie in the AB plane and were mainly oriented along the so-called A direction. A schematic drawing of how the specimens were cut from the board and the nomenclature used is shown in **Figure 3**.

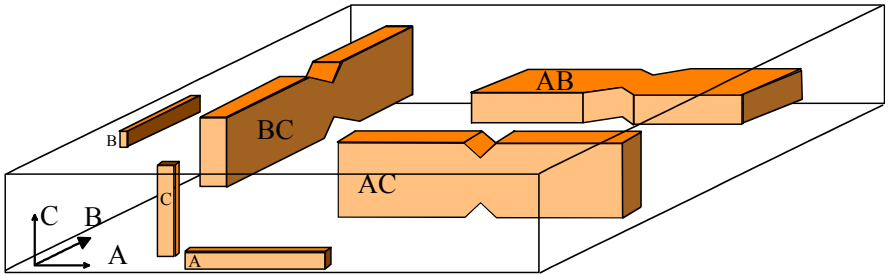

Figure 3: Denominations of sample orientation in the material. Samples denoted A, B and C were used for tensile measurements while those denoted AB, AC and BC where used in shear experiments.

3.2 Spruce wood

Samples were prepared from mature never-dried wood of Norway spruce (*Picea abies*), stored at about −25 °C. The specimens were kept at 70 % RH until tested. The wood material was treated as being orthotropic with the principal material axes corresponding to: the tangent to the growth ring (T), the direction of the rays (R), and the longitudinal axis of the tree (L). The shear and compression specimens were cut along the radial tangential (RT) direction of the material. The orientation of the samples with respect to wood structure is shown in **Figure 4**.

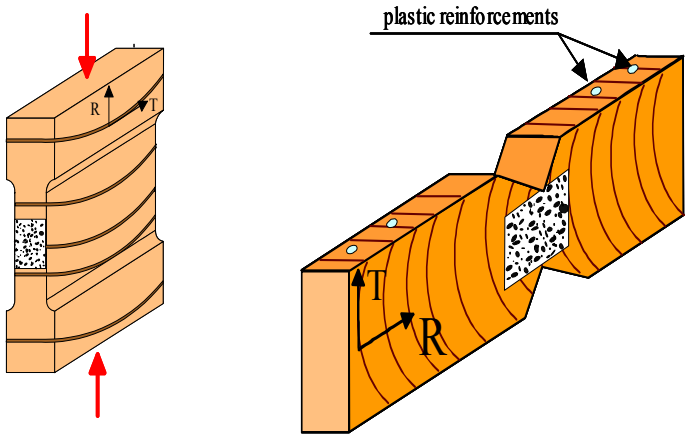

Figure 4: Orientations of the test specimens used in the pure compression (left) and combined shear and compression (right) tests. R and T refer to the radial and the tangential direction of wood, respectively.

4 Methods

4.1 Digital Speckle Photography

Digital Speckle Photography (DSP) was used to measure the displacement field on one face of the specimen. The specimen's surface was first painted with a white paint and thereafter sprayed with a black paint to obtain a characteristic pattern as shown in **Figure 5**. The DSP measurement technique monitors the manner in which the random speckle pattern, attached to the specimen surface, is displaced when the specimen is loaded. Deformation over the whole field is determined using a digital image correlation algorithm that analyzes the imagines of the pattern taken with a CCD camera before and during the test. Both the displacement and the strain distributions can be mapped (Sjödahl 1995).

The shear strain γ_{xy}, the longitudinal normal strain ϵ_x and the transverse normal strain ϵ_y were calculated by differentiation according to **Equation 1** where δx and δy are the distances between neighboring points in the x and y directions, respectively, and u and v are the displacements in the x and y directions, respectively, with i and j as the coordinates of the points. The strain fields at the different load levels were obtained by differentiation of the displacement field obtained from the first image (under zero load) and the

subsequent images under increasing load. Images were taken for each load increment of 10 N.

$$
\begin{aligned}
\frac{\Delta u}{\Delta x}(i,j) &= \frac{u(i+1,j)-u(i,j)}{\Delta x} \\
\frac{\Delta u}{\Delta y}(i,j) &= \frac{u(i,j+1)-u(i,j)}{\Delta x} \\
\frac{\Delta v}{\Delta y}(i,j) &= \frac{u(i,j+1)-v(i,j)}{\Delta y} \\
\frac{\Delta v}{\Delta x}(i,j) &= \frac{v(i+1,j)-v(i,j)}{\Delta x} \qquad \text{with} \qquad \begin{aligned} i &= 1\cdots 15 \\ j &= 1\cdots 15 \end{aligned} \\
\epsilon_{xx}(i,j) &= \frac{\Delta u}{\Delta x}(i,j) \\
\epsilon_{yy}(i,j) &= \frac{\Delta v}{\Delta y}(i,j) \\
\gamma_{xy}(i,j) &= \frac{\Delta v}{\Delta x}(i,j) + \frac{\Delta u}{\Delta y}(i,j)
\end{aligned}
\tag{1}
$$

It should be noted that, when working with a fixed camera, the area under the first image was not the same as the area under one of the subsequent images due to translation. Considering both areas as the same original area introduced a small bias. The area covered by the camera was 13.5 by 13.5 mm. At the borders of the images, however, the data are more susceptible to errors so that the area analyzed was in reality slightly smaller being about 10 by 10 mm.

For the pure compression test, the average stress σ_R in the section of interest was defined as the compression force divided by the cross-sectional area of the specimen, that is the ideal theoretical stress. The radial elastic modulus E_R was defined as the ratio of the average compression stress σ_R to the average compression strain value ϵ_R in the section of interest.

For the pure shear test, the average shear stress between the notches τ_{xy} was defined as the shearing force divided by the cross-sectional area of the specimen, that is a uniform shear stress distribution between the notches was assumed. The shear modulus G_{xy} was defined as the ratio of the average shear stress τ_{xy}, to the average shear strain γ_{xy}.

For the combined shear and compression test, both for the MDF and for the wood material, the average stress between the notches τ_{xy} and G_{xy}

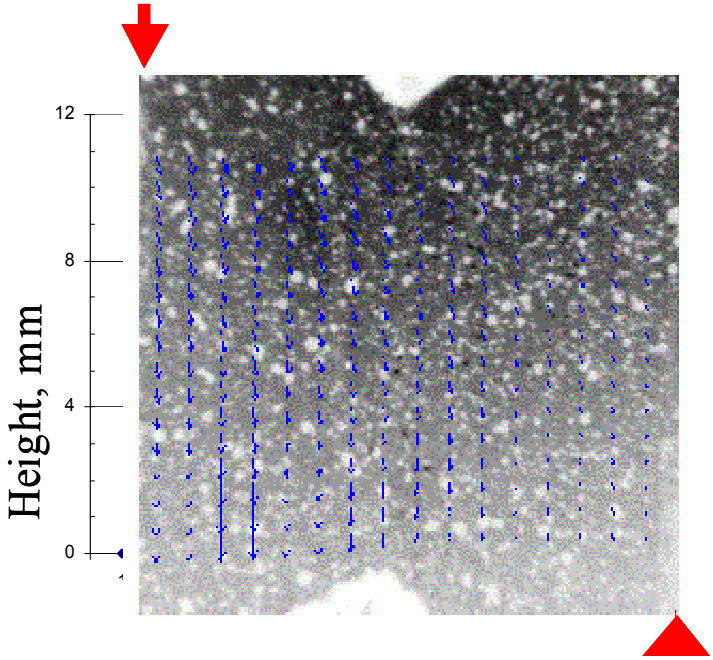

Figure 5: Speckle pattern and the superimposed displacement field for the section between the notches of a sample subjected to simple shear.

was defined as in the pure shear test case. The stress field in the region of interest was approximated to an ideal uniform stress field, which was centered between the notches going from one notch to the other and being about 10 mm wide.

4.2 Experimental methods

All the tests were performed at room temperature in a tensile testing machine (MTS) under a controlled crosshead displacement. A standard 500 N MTS load cell was used to measure the applied force. Digital Speckle Photography (DSP) was used to record the displacement field under the test by taking images at every 10 N interval, when the movement was temporarily halted.

4.2.1 Tests in tension and in compression

MDF samples were loaded in tension to fracture and the linear part of the response was used to calculate the elastic moduli in the three main directions. The shape and orientation of the sample are shown in **Figure 3**.

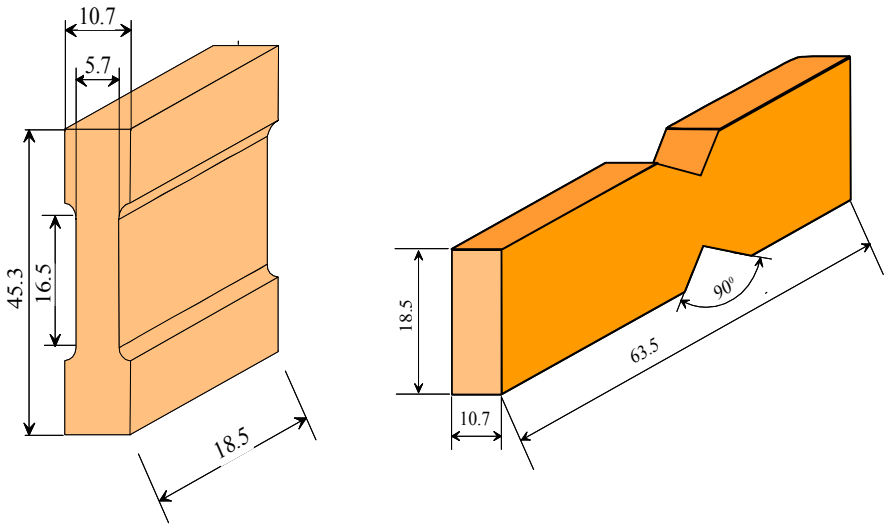

Figure 6: Dimension of the test specimens used in the pure compression (left) and combined shear and compression (right) tests. Dimensions are in mm.

The dependence of the elastic modulus on wood density was investigated by testing wood in compression in the radial direction. About twenty samples were tested in radial compression to a load of 100 N (1 MPa). The cross-head displacement during the test was 0.2 mm/ min. Density profiles were measured on the compression specimens using X-ray densitometry (Tongli et al. 1999), three specimens were tested. The pure compression test specimens were dog-bone shaped (**Figure 6** (left)).

4.2.2 Pure shear and combined shear and compression tests

Notched specimens were used in both the pure shear and in the combined shear and compression tests. A 90 ° notch was milled to a depth of 3.5 mm on each side of the specimen. The length and width of the specimens are fixed standard dimensions for the Iosipescu shear test device (ASTM D 5379-93). In order to prevent local compression of the specimens in the region of gripping two plastic rods were introduced, in both the griping sections, in the vertical direction. **Figure 6** (right) shows the size for the test specimens.

Tests in pure shear were performed on the MDF using the Wyoming version of the Iosipescu shear test fixture. The left-hand jaw was set on a slide guide and was thus free to move along the direction of the longitudinal

axis of the specimen (**Figure 1**). The specimens were loaded to a maximum load of 60 N. The average stress in the cross section at 60 N was about 0.42 MPa, that means that the tests were performed in the elastic range of the material.

Tests in combined shear and compression were performed on both materials using the in-house modified Iosipescu device. The rotation angle of 45 ° was used. The load was applied to a maximum of 80 N corresponding to 1 MPa of stress in compression in the section between the notches. This stress level was chosen in order to keep the test in the elastic range of the material.

5 Finite Element analysis

In order to increase confidence about the results obtained with the new shear and compression device a Finite Element (FE) model of the tests was developed together with the measurements. The commercial FE-code ABAQUS/Standard, version 6.3 was used (Hibbit et al. 2002).

5.1 Development of the model (MDF characteristics)

The model has been developed using the characteristic for MDF. First the material model has been checked in simple shear and then the model has been tested in shear and compression to study which angle of rotation gave the most uniform strain field.

5.1.1 Simple shear

The first step of the FE modeling was to examine a sample subjected to simple shear. The device used in the present analysis was the modified Wyoming device which introduces the load in a manner that is represented by displacements applied to the loading blocks. A model with asymmetric loading blocks was studied. This model was close to those used by Ho et al. (1993) and by Grédiac et al. (1994).

In the 2-D model, which is shown in **Figure 7**, linear four-node brick elements were used. The loading blocks were modeled as isotropic linear elastic material, with E =200 GPa and $\nu = 0.3$.

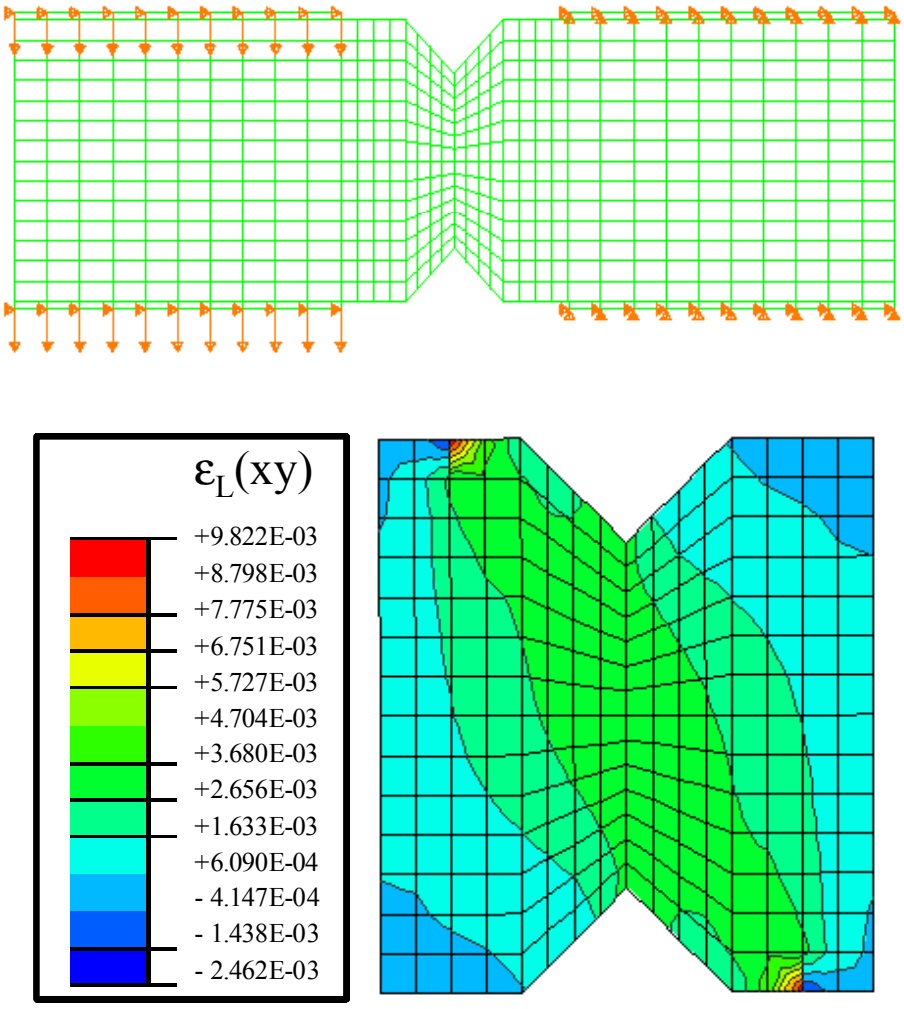

Figure 7: Model for the FE analysis of the shear test (up) and results for the strain fields (down).

Table 1: Material parameters chosen for the model of the MDF material. The Young's and shear moduli are given in MPa.

	E_B	E_C	E_A	G_{BC}	G_{BA}	G_{CA}	ν_{BC}	ν_{BC}	ν_{CA}
MDF	3200	50	3400	58	68	64	0.5	0.45	0.008

The first material used in the model is an isotropic linear elastic material (E =3370 MPa, ν =0.43). A friction coefficient of 0.3 was introduced between the loading blocks and the sample itself. The friction model in ABAQUS is an extended version of the classic isotropic Coulomb friction. The analysis was non-linear due to the friction in the contact area. The shear field obtained has the same shape as that found in the literature (Xing et al. 1993).

The model was then developed to a 3-D model. The thickness of the loading blocks was the same as for the sample. In the 3-D model, shown in **Figure 8**, linear eight node brick elements were used.

The model was then developed to an orthotropic linear elastic material. This was based on the nine characteristic material constants calculated or obtained from measurements of pure tensile and pure shear load, see **Table 1**.

The Poison's ratios, ν_{ij}, have the physical interpretation of characterizing the transverse strain in the j direction. In general ν_{ij} is not equal to ν_{ji} but related according to:

$$\frac{\nu_{ij}}{E_i} = \frac{\nu_{ji}}{E_j} \quad (i \neq j, \text{ no summation}) \tag{2}$$

Material stability requires:

$$|\nu_{ij}| = \frac{E_i}{E_j} \quad (i \neq j, \text{ no summation}) \tag{3}$$

The elastic moduli of the MDF were almost the same in the A and B directions but the shear moduli shows that the material has to be considered as an orthotropic. With the model the three different orientations, AC, AB and BC (see **Figure 3**) were analyzed.

An initial displacement of 0.01 mm was applied to the blocks to simulate the gripping of the sample. The displacement, which was applied to the loading blocks on the left-hand side of the sample, was increased in three

Table 2: Displacement values applied in the shear and compression model for the MDF. Those are related to the forces applied in the test (N is the compression force and T is the shear force).

Total applied force (N)	**Forces** (N)		**Displacements** (mm)	
	N	**T**	**u**	**v**
0 ° **(pure shear)**	0	80	0	−0.13
30 °	40	72	0.03	−0.12
45 °	56	56	0.04	−0.09
60 °	72	40	0.05	−0.06
90 °**(pure compression)**	80	0	0.06	0

subsequent steps. The values of the applied displacements in the steps were the experimental displacements reached at loads of 40 , 60 and 80 N, respectively. The values of the displacements were related to the orientation of the material so different displacements were applied in the three cases.

5.1.2 Combined shear and compression

The aim of this study was to test the behavior of wood subjected to shear in the radial-tangential plane and to compression in the radial direction. In the combined shear and compression model, only the BC orientation of the MDF material was studied, as this orientation better represents the radial-tangential orientation of wood. The term "rotation" is used to indicate a rotation of the device, while the term "orientation" is used to indicate the orientation of the MDF material of the specimens. The different rotations were represented in the analysis by the application of different displacements in x and y. The displacements were calculated by the Elasticity Theory (equations of equilibrium and of compatibility) to give the strain field related to the applied force. The values of the displacements applied in the different cases are listed in **Table 2**.

As before, an initial displacement of 0.01 mm was applied to the blocks, in the y direction, to simulate the gripping of the sample. Thereafter, displacements in the x and y directions were applied to the loading blocks on the left side. The edges on the right side of the sample were constrained in two directions, meaning that the right lateral edge was constrained along x while the left lateral edge was given the same displacement, along x, as the one applied to the nodes of the loading blocks on that side (**Figure 8**). This was done to represent the real testing conditions of the sample subjected to combined shear and compression as can be seen from **Figure 2**.

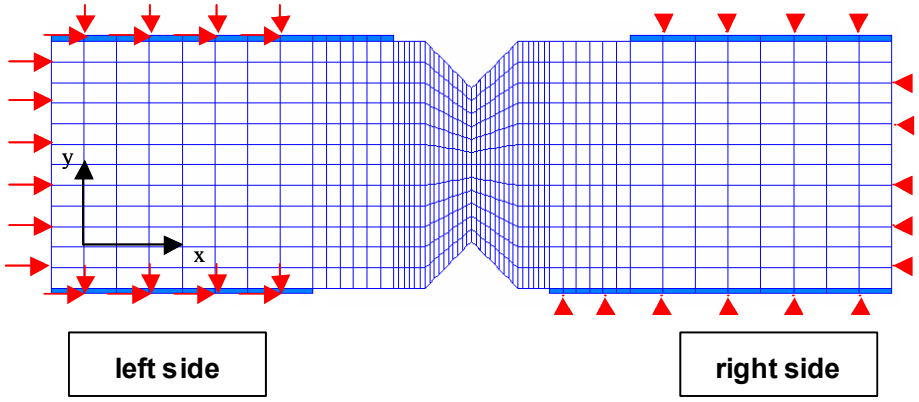

Figure 8: Model with the applied displacements and constraints for the Finite Element Analysis of the combined shear and compression test (the initial gripping displacements are not shown). The mesh shown was used for the model of wood material.

In the non linear analysis the strains are given as logarithmic strain:

$$\epsilon_L = ln(1 + \epsilon_N) \tag{4}$$

where ϵ_N is the normal strain (ϵ_{xx}, ϵ_{yy} and γ_{xy}) defined as in **Equation 1**. For the small displacements here analyzed these strains are about equal.

5.2 Model of the wood material

For wood, the model was improved with a thicker division of the mesh in the middle section. Boundary conditions as in the preceding model were used. The values of the displacements applied in this analysis, at the various steps, are listed in **Table 3**. They represent the displacements reached in the test at the applied loads of 20 , 40 , 60 and 80 N, respectively. Those values of displacement were in agreement with the registered crosshead displacement of the MTS when testing the wood. The material constants of the wood as listed in **Table 4** were used in this calculation.

5.2.1 Material models

The mechanical properties of wood are generally determined considering wood as a homogeneous material. Not much experimental work has been

Table 3: Displacement values applied in the shear and compression model for wood. Those are related to the forces applied in the test at a 45 ° rotation. N is the compression force and T is the shear force.

Total applied force (N)	**Forces** (N)		**Displacements** (mm)	
	N	**T**	**u**	**v**
−1 ° **(gripping)**	0	−1	0	−0.00007
−20 °	−14.1	−14.1	−0.005	−0.02
−40 °	−28.3	−28.3	−0.01	−0.04
−60 °	−42.4	−42.4	−0.015	−0.06
−80 °	−56.6	−56.6	−0.02	−0.08

Table 4: Material parameters chosen for the FE analysis when regarding wood as an orthotropic homogeneous wood material. The Young's and the shear moduli are given in MPa and the density is given in kg/dm^3.

	E_R	E_T	E_L	ν_{RT}	ν_{RL}	ν_{TL}	G_{RT}	G_{RL}	G_{TL}	ρ
orthotropic	1000	850	12500	0.61	0.034	0.028	60	600	565	0.5

carried out to determine the variation of the properties within the growth ring of the wood. In order to model the wood as an orthotropic homogeneous material the material constants specified in **Table 4**, calculated as described below, were used.

These values, listed in **Table 4**, are based on general data for wood (Carrington 1923, Jernkvist 2000, Persson 2000) adjusted to the following general relations established for spruce wood (Bodig and Jayne 1982):

$$E_L : E_R : E_T \cong 20 : 1.6 : 1 \tag{5}$$

$$E_L : G_{RL} \cong 14 : 1 \tag{6}$$

The strength and stiffness of wood are considerably greater in the longitudinal than in the perpendicular direction. This is easily understood since 90-95% of the fibers are oriented longitudinally. There is also a difference in properties between the radial and tangential directions. This is probably due to differences between the structural arrangements of the wood fiber and to the presence of ray cells (Persson 2000).

The components of the shear moduli have been matched according to the following relation established by Holmberg (1998):

$$G_{RL} : G_{TL} : G_{RT} \cong 10 : 9.4 : 1 \tag{7}$$

The values calculated for the transverse shear modulus G_{RT} were in agreement with experimental values found by Dumail et al. (2000).

Annual ring variation To obtain a proper model for the annual ring structure of the wood, it was divided into zones of earlywood, transitionwood and latewood. Earlywood usually has a non-linear elastic response when subject to large compression forces perpendicular to the grain (Holmberg 1998), however as the tests were here made in the elastic range of the material a linear elastic response was chosen. Both latewood and transition wood have linear elastic behavior as long as no cracks are developed.

Using the same relations as listed above **(Equations 2, 3, 5–7)** the constants for the annual ring structure have been calculated from experimental data. The different zones of earlywood, transitionwood and latewood were characterized by their density and are based on those experimental data (Ando and Ohta 1995, Jernkvist 2000). The values for the transverse elastic modulus E_R were based on the experiments performed in compression in this study. The values for the elastic transverse modulus E_T were in agreement with the experimental values found by Bergander and Salmén (2000). All the values are in agreement with the ones found in the literature (Koponen et al. 1991, Farruggia and Perré 2000). The same relation between wood density and longitudinal elastic modulus E_L can be found in a study of Persson (2000). The values listed in **(Tables 4 and 5)** are still probable estimates rather than definite values.

Annual ring model In this model the width of every annual ring was set to 6.05 mm and was divided into five equal layers. Three of those layers were assigned to the earlywood region, one to the transitionwood and one to the latewood region, respectively. In this way the section between the notches was modeled to have six annual rings (see **Figure 9**). The material of this section was modeled with the characteristic constants as listed in **Table 5**. The material of the gripped parts of the sample was modeled with the characteristic constants of the "orthotropic homogeneous" wood as listed in **Table 4**. The growth rings in the specimens used in the combined shear and compression tests were about 1 to 2 mm wide and there were about 12 annual rings in the section between the notches. However the model was still considered accurate enough to represent the general behavior of the sample under shear and compression load.

Table 5: Material parameters chosen for the elastic properties of dry wood (12% moisture content). The Young's and the shear moduli are given in MPa and the density is given in kg/dm^3.

	Early-wood1	**Early-wood2**	**Early-wood3**	**Transition-wood**	**Late-wood**
ρ	0.21	0.28	0.35	0.42	0.6
E_R	600	730	805	1020	1280
E_T	395	475	610	860	1190
E_L	7700	9125	10060	12750	16000
ν_{RT}	0.75	0.77	0.65	0.59	0.53
ν_{RL}	0.037	0.039	0.036	0.034	0.032
ν_{TL}	0.026	0.025	0.027	0.028	0.029
G_{RT}	36	40	45	65	75
G_{RL}	360	400	450	650	750
G_{TL}	340	375	420	600	705

6 Results from the numerical analysis

6.1 Results from the study on the MDF

6.1.1 Finite Element model in simple shear

A comparison of the results for the three orientations shows that the AB orientation was the one that showed the most uniform strain field in the section between the notches, while the other two orientations gave strain fields

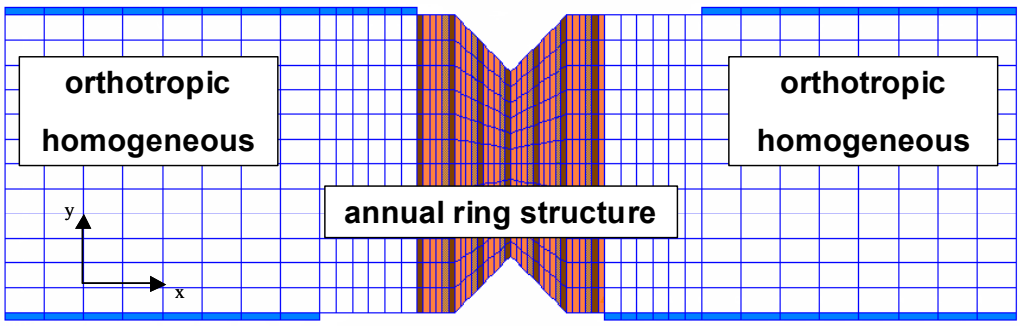

Figure 9: Material distribution in the model with the annual ring structure.

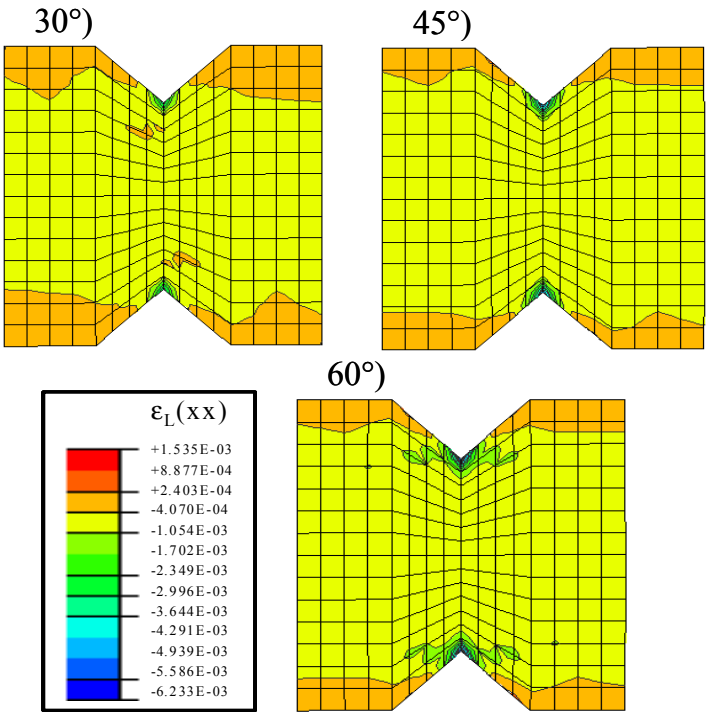

Figure 10: Compression strain field of the model at 30 °, 45 ° and 60 °. BC orientation of the MDF material.

that were uniform even if there was a strain concentration at the peak of the notches. The orientation BC was the one closest to a possible characterization of wood tested in the radial-tangential direction. For this reason it is important to note that the strain field in that orientation was still quite uniform.

6.1.2 Finite Element model in combined shear and compression

In the combined shear and compression model only the BC orientation of the material was studied. Three different rotations of the sample were analyzed: 30 °, 45 ° and 60 °.

As can be seen in **Figure 10**, the compression field in the 60 ° and 30 ° rotations were not completely uniform in the section between the notches. In the 45 ° rotation, the compression strain field was uniform in the section between the notches but had maximum and minimum values near the pitches of the notches. This is due to the shape of the sample itself.

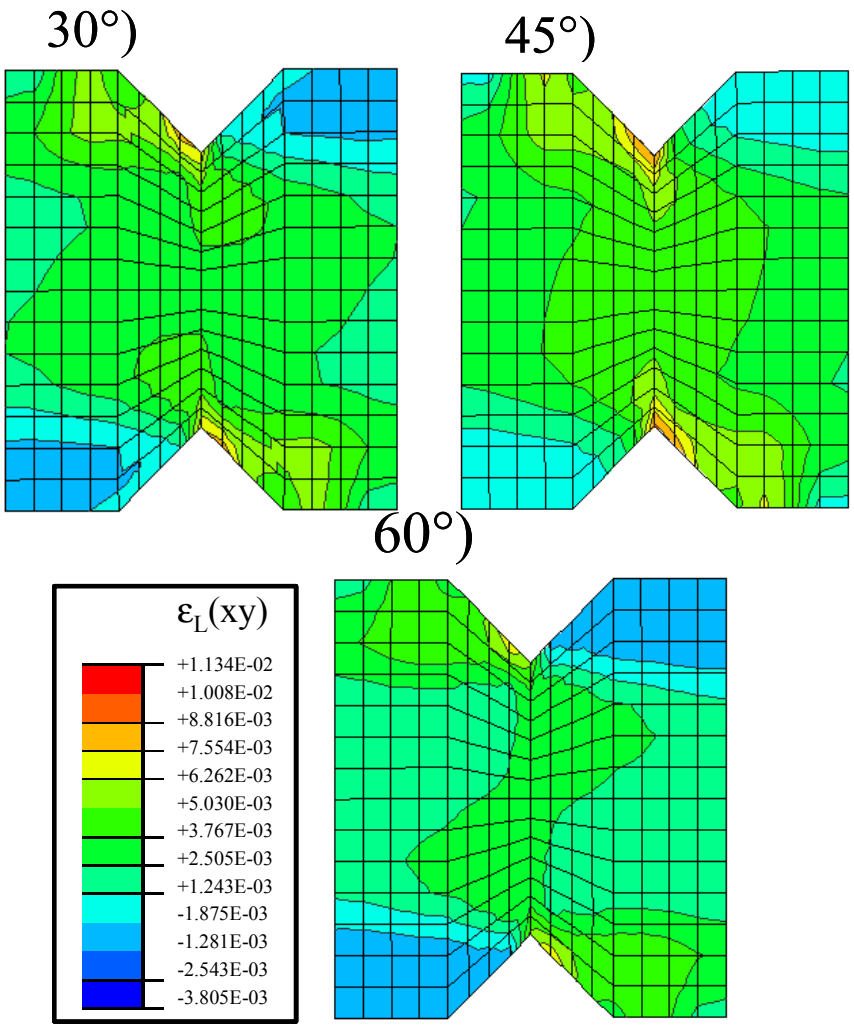

Figure 11: Shear strain field of the model at 30 °, 45 ° and 60 °. BC orientation of the MDF material.

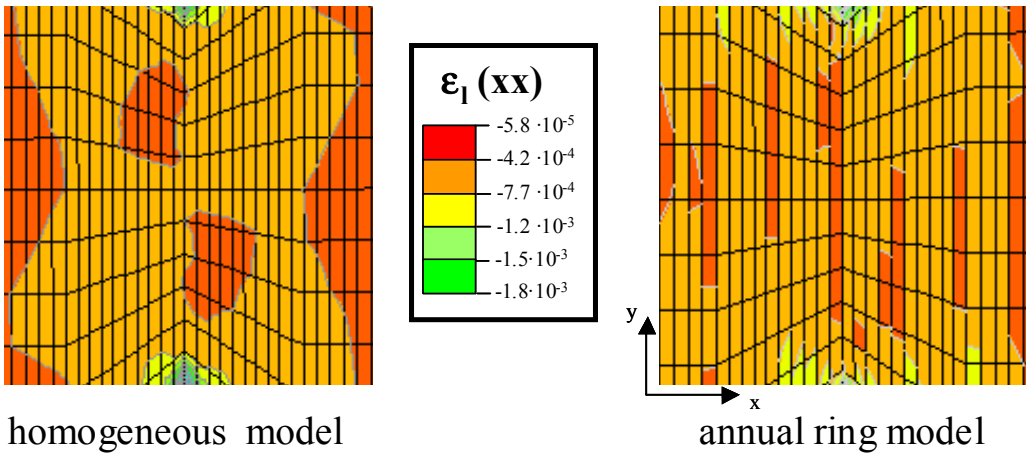

Figure 12: Compression strain fields from the Finite Element analysis with wood as an orthotropic homogeneous linear elastic material (left) and as a material with an annual ring structure (right).

The strain shear field was, as seen in **Figure 11**, almost uniform for the 45 ° rotation. The rotation of 45 ° was the only configuration for which both shear and compression fields were almost uniform in the section of interest. For this reason the 45 ° rotation was chosen to measure deformation with samples in the BC orientation.

6.2 Model with orthotropic homogeneous wood and with the annual ring structure

Under the same load and boundary conditions, the deformation of two material models were analyzed: one with an "orthotropic homogeneous wood structure" and the other with the annual ring structure with variable properties.

In **Figure 12**, the resulting compression strain fields from the numerical analysis are shown for both the materials modeled. In the annual ring model the strain distribution was more influenced by the differences in modulus of the material in the annual ring than from its position in the section.

The resulting shear strain fields are shown, in **Figure 13**, for both the models. The shape as well as the values of the shear strain was influenced by the structure of the material in the model. The strain in the earlywood, in the annual ring model, was about 10 times larger than the strain in the latewood.

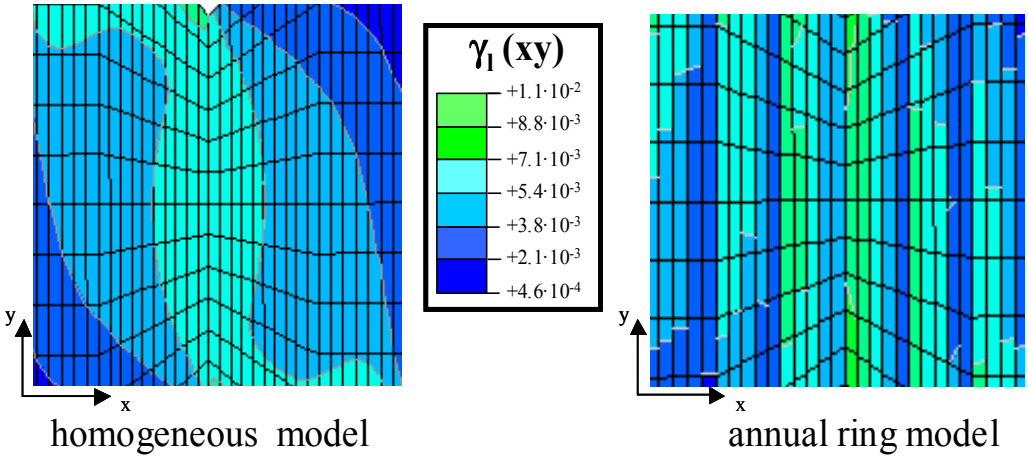

Figure 13: Shear strain fields from the Finite Element analysis with wood as orthotropic homogeneous linear elastic material (left) and as material with annual ring structure (right).

7 Experimental results

Combined shear and compression tests on dry wood
For the combined shear and compression test measurements with the modified Iosipescu device in 45 ° rotation were performed. The strain fields in the section between the notches are shown in **Figure 14** where ϵ_n and γ_n are the normal strains defined as in **Equation 1**. The diagrams show the results from one test, at the maximum load applied (80 N). The displacements shown are the average values of five tests with a standard deviation of less than 0.05.

The strain in the x direction is mainly due to the load in compression. A rather uniform strain field within the section was seen despite the annual ring structure. This is probably due to a too low resolution as a result of the small strains. The strain in the y direction is instead mainly due to the shear load and gave a less uniform strain field. In this case in fact, it is possible to see a reflection of the structure in the strain field in the annual ring. In the section analyzed there were about six annual rings.

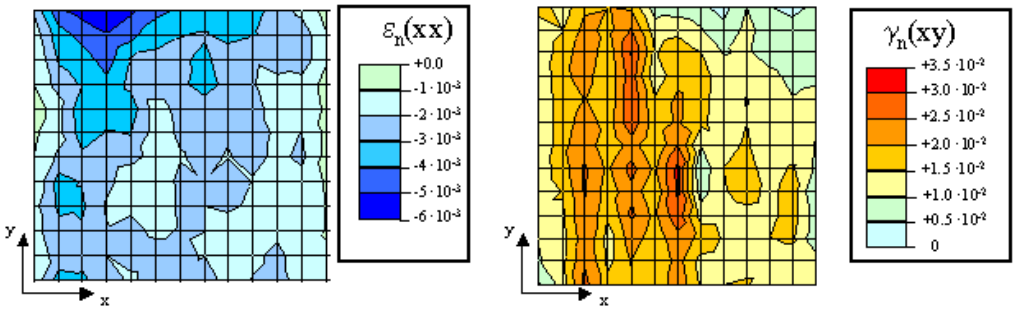

Figure 14: Compression (left) and shear (right) strain fields results from a combined shear and compression test at 45 ° rotation for spruce wood at 12 % moisture content.

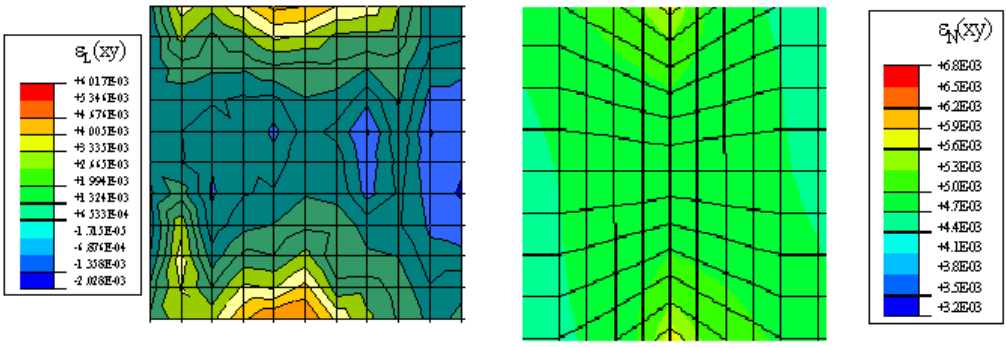

Figure 15: Comparison of the shear field in the section between the notches for the DSP results (left)and from the FE model (right) in case of the BC orientation.

8 Discussion

8.1 Study of the MDF material

8.1.1 Simple shear

From the FE analysis, it is evident that the maximum strain for the Iosipescu test device was obtained in the section between the notches in the case of an orthotropic material in all the orientations tested. As stated in the introduction, the area in which the strain field was supposed to be constant was about 2.5 mm wide.

The influence of the stress concentrations at the notches was visible in

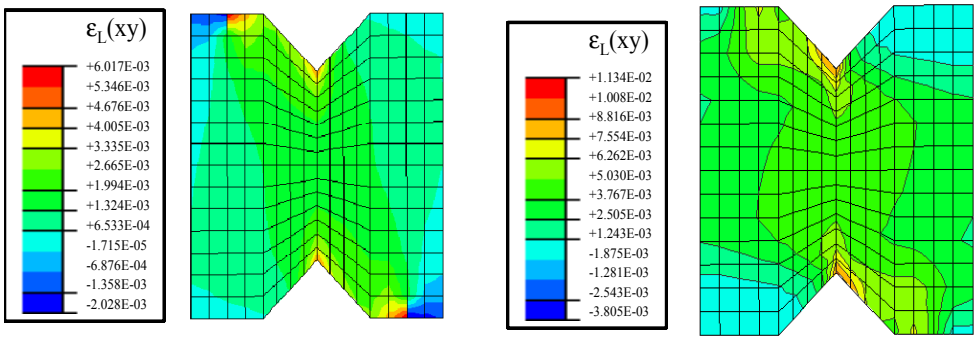

Figure 16: Shear strain field of the model in simple shear (left) and from the model at 45 ° (right).

the image, as can be seen in **Figure 15**. In the BC orientation, as in the other orientations, the modeled average strain of ϵ_L was about the same as that found experimentally. The shape of the strain field was also in quite good agreement.

The shear strain patterns in the case of pure shear and of combined shear and compression forces were not similar as can be seen in **Figure 16**. This can be due to the fact that, in the modified device, the left–hand jaw is not free to move along the longitudinal direction of the sample. The shear in the section between the notches was however still almost uniform and the values of the shear strain were similar in the two cases. In the following, experimental results obtained with an applied force of 80 N (0.7 MPa) and analytical results obtained with the displacement related to that force are compared (see **Table 2**).

As can be seen in (**Figures 17 and 18**), the displacement fields, as well as the strain fields, were in quite good agreement. The strain field in compression is almost a degree of magnitude smaller than that in shear. This is due to the fact that the material is stiffer in that direction and to the fact that the component of shear deformation along x is in this direction opposite to those due to compression, i.e. the two loads have opposite effects.

8.2 Discussion from the study on dry wood

For wood, the shapes of the displacements fields from the experimental and analytical results were very similar. The displacements in both the models were a linear combination of the displacements due to pure shear and pure

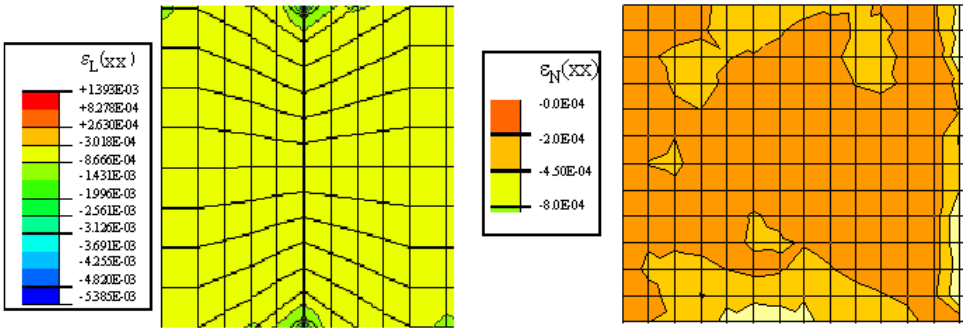

Figure 17: Comparison of the compression strain field in the section between the notches in the FE model (left) and from the DSP results (right) with a 45 ° rotation.

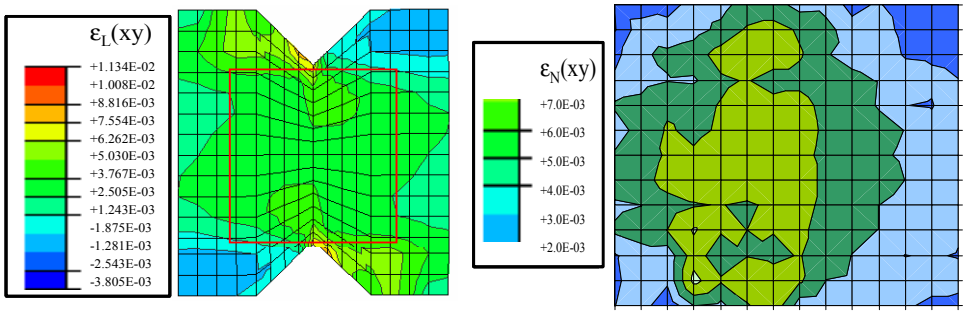

Figure 18: Comparison of the shear strain field in the section between the notches in the FE model (left) and from the DSP results (right) with a 45 ° rotation.

compression. The values of shear strain, from the analysis and from the experiments, were similar (**Figures 13 and 14**). On the other hand the compression strain field (**Figure 12**) had values about one order of magnitude inferior to the experimental ones. This can probably be due to a collapse of wood cells occurring at a lower strain level than expected.

To check whether a plastic collapse had occurred during combined shear and compression test, the same samples were subjected to compression. These compression tests revealed that the wood material had the same elastic modulus as the wood not subjected to shear and compression. This means that if a collapse had occurred during the combined shear and compression test, this had been in the elastic range of the material and that the wood had recovered completely from that shear and compression load.

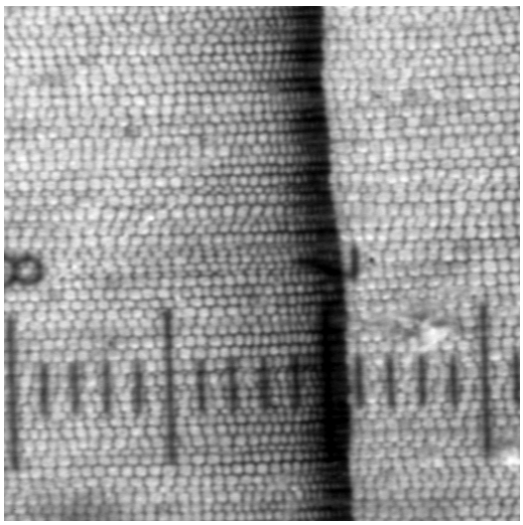

Figure 19: Annual ring in the section between the notches. The area is 1.6 by 1.6 mm The specimen was loaded to 160 N (1.3 MPa).

An attempt to visually observe the wood cell collapse under the combined load was made. Tests with the same relation of combined shear and compression load, up to a maximum load of 160 N, were performed with special attention to the single cell deformation. The deformation of the annual ring in its width was followed with a microscope with an x100 magnification. The deformation was however still too small (0.5 mm) to be detected. No local collapse of fibers could be seen, as illustrated in **Figure 19**. Collapse would have been expected to develop in the first cell rows of the earlywood.

9 Conclusions

These analyses have shown that the FE model truly represents the behavior of the MDF material subjected to shear in testing in an Iosipescu modified shear test device. This has made it possible to examine the strain field in the whole sample and to decide that the best configuration to use in the new device was a 45 ° rotation. The comparison between the experimental and the analytical results shows that the new device is sufficiently accurate to enable the behavior of an orthotropic material subjected to combined shear and compression loads to be studied. The main design idea of the new device is valid.

In combined shear and compression tests on dry wood, the values of the strain field in compression were found to be ten times larger in the experi-

ments than in the analytical results. The probable reason for this is a local collapse of earlywood fibers. This means that a combined shear and compression load would be favorable to facilitate collapse of wood. However this deformation was completely elastic. The Finite Element analysis, with the material model as a linear elastic material, was thus not able to predict that behavior even though a variation of properties of the material in the annual ring structure was introduced.

10 Future work

A microscopy study on the collapse of the wood cells under combined shear and compression load could help in understanding the behavior of the wood fiber during the mechanical pulping process.

The new device developed in this study is based on a shear test method that uses a notched sample. This sample geometry is not optimal for testing compression due to the stress concentration that is created at the pitch of the notches themselves. Moreover the sample has a surface that is too large to be studied under a microscopy: the section between the notches has a displacement under load greater than the image possible to view by microscopy if the cell structure should be studied. To have a good resolution the surface must be cut with a microtone, i.e. the sample must be cut using a different method than that used in this study.

Another kind of test should be designed to test small (few annual rings) samples of wood under combined shear and compression load.

Acknowledgments

My supervisor Dr. Lennart Salmén is gratefully acknowledged for valuable scientific guidance and advice.

Thanks to Dr. Mikael Sjödahl from the Division of Experimental Mechanics of Luleå University of Technology for lending the DSP software.

Thanks to Dr. C. Hörnell for the linguistic revision of the manuscript.

Many people at STFI have helped me during those years. Especially I would like to thank: Petri Mäkelä for reading the manuscripts and giving sensible and valuable comments; Sune Karlsson for helping me dealing with the MTS; Leif Falk for his help in cutting the samples and building the modification for the testing device; everyone in the Wood and Fiber Physics group for all their friendship and valuable discussions; the other Italians, Marco Lucisano and Orlando Girlanda, for support and helpful discussion in an easy language.

Thanks to Prof. Anders Eriksson and the entire group at Mekanik, KTH, for fast and reliable answers every time I needed their advice.

Thanks to my parents because without their support and endless patience during my long studies I would never have been even an engineer.

Bibliography

Adams D.F. and Walrath D.E. (1987) Further development of the Iosipescu shear test method. *Exp Mech* **27**:113–19.

Ando K. and Ohta M. (1995) Variability of fracture toughness by the crack tip position in an annual ring of coniferous wood. *J Wood Sci* **45**(4):275–286.

Arcan M., Hashin Z. and Volosin A. (1978) A method to produce uniform plane-stress states with applications to fiber-reinforced materials. *Exp Mech* **18**(4):141–146.

Bansal A. and Kumosa M. (1995) Application of the biaxial Iosipescu method to mixed-mode fracture of unidirectional composites. *Int J Fract* **71**:131–150.

Bergander A. and Salmén L. (2000) The transverse elastic modulus of the native wood fibre wall. *J Pulp Pap Sci* **26**:234–238.

Bodig J. and Jayne B. (1982) *Mechanics of Wood and Wood Composites.* New York, USA.

Carrington H. (1923) The elastic constant of spruce. *Phil Mag S.6.* **45**(269):1055–1057.

Conant N.R. and Odom E.M. (1995) An improved Ioipescu shear test fixture. *J Compos Technol Res* **17**:50–55.

Dumail J.-F., Olofsson K. and Salmén L. (2000), An analysis in rolling shear of spruce wood by the Iosipescu method. *Holzforschung* **54**:420–426.

Farruggia F. and Perré P. (2000) Microscopic tensile tests in the tranverse plane of earlywood and latewood parts of spruce. *Wood Sci Technol* **34**:65–82.

Feldman A., Tasi J. and Stany D.A. (1966) Experimental determination of stiffness properties of thin-shell composite cylinders. *Exp Mech* **8**:385–394.

Grédiac M., Pierron F. and Vautrin A. (1994) The Iosipescu in-plane shear test applied to composites: A new approach based on displacements field processing. *Comp Sci & Technol* **51**:409–417.

Hibbit, Karlsson and Sorensen (2002) *ABAQUS/Standard User's Manual*, version 6.3, Hibbit, Karsson & Sorensen Inc., Rhode Island, USA.

Ho H., Tsay M.Y., Morton J. and Farley G.L. (1993) Numerical analysis of the Iosipescu specimen for composite material. *Comp Sci & Technol* **46**:115–128.

Holmberg S. (1998) A numerical and experimental study of initial defibration of wood. PhD thesis, Division of Structural Mechanics, Lund Institute of Technology, Lund, Sweden.

Iosipescu N. (1967) New accurate procedure for single testing of metals. *J Mater* **2**:537–566.

Jernkvist L.O. (2000) On the fracture behaviour of softwood. PhD thesis, Division of Solid Mechanics, Luleå University of Technology, Luleå, Sweden.

Koponen S., Toratti T. and Kanerva P. (1991) Modelling elastic and shrinkage properties of wood based on cell structure. *Wood Sci Technol* **25**:25–32.

Liu, J.Y. (1984) New shear strength test for solid wood. *Wood Fiber Sci* **16**(4):567–574.

Liu J.Y. (2000) Effects of shear coupling on shear properties of wood. *Wood Fiber Sci* **32**:458–465.

Liu J.Y., Flach D.D., Ross R.J. and Lichtenberg G.J. (1999) An improved shear test fixture using the Iosipescu specimen. *Mech Cellul Mater AMD-VOI 231/MD-VOI* **85**:139–147.

Persson K. (2000) Micromechanical modelling of wood and fibre properties. PhD thesis, Division of Structural Mechanics, Lund Institute of Technology, Lund, Sweden.

Sjödahl M. (1995) Electronic Speckle Photography applied to In-plane Deformation and Strain Field Measurements. PhD thesis, Division of Experimental Mechanics, Luleå University of Technology, Luleå, Sweden.

Tongli W., Aitken A.N., Rozemberg P. and Carlson M.R. (1999) Selection for the height growth and pilodyn pin penetration in lodgepole pine: Effects on growth traits, wood properties, and their relationships. *Can J Forest Res* **29**:434–445.

Walrath D.E. and Adams D.F. (1983) The Iosipescu shear test as applied to composite materials. *Exp Mech* **23**:105–110.

Xing Y.M., Poon C.Y. and Ruiz C. (1993) A whole-field strain analysis of the Iosipescu specimen and evaluation of experimental errors. *Comp Sci & Technol* **47**:251–259.